Original Research Article

Efficacy Analysis of Corneal Photo-vitrification (CPV) for Improved Vision of Age-related Macular Degeneration (AMD) Eyes

ABSTRACT

Purpose: To analyze the safety and efficacy of corneal photovitrification (CPV) for improved visions of age-related macular degeneration (AMD) eyes.
Study Design: Using CPV for improved visions of AMD eyes.
Place and Duration of Study: New Taipei City, Taiwan, and Austin, TX, USA; between April, 2022 and June, 2022.
Methodology: The CPV efficacy is calculated based on the rate equation given by dM/dt=-k(t) M(t), where M(t) is the PCV-treated corneal stroma; and k(t) is the rate coefficient given by an Arrhenius formula, $k(t) = A_0 \exp[-Ea/(RT(t,z)]$, where t and z are the laser irradiation time and depth of the cornea stroma; Ea is the activation energy and R is the gas constant. The temperature spatial and temporal profiles are given by the numerical solutions of a heat diffusion equation with a volume heating source. Various effective depths including the tissue damage depth, temperature penetration depth and conversion depth, governed by the tissue absorption coefficient, light intensity and dose (or irradiation time), and the related threshold values, are introduced in replacing the conventional penetration depth based on a Beer's law.
Results: The suggested protocol for CPV treatments include: a diode laser at about 2 μm wavelength (with absorption coefficient about 100 cm^{-1}). The laser dose is about 25 J/cm^2/spot and irradiation time of 150 ms.
Conclusion: The efficacy of CPV may be predicted/calculated by our modeling based on rate equation and the corneal stroma temperature rise due to laser heating. The preferred retinal locus (PRL) movement observed post-CPV is caused mainly by neuroadaptation.

Keywords: cornea stroma, diode laser heating, photo-conversion efficacy, vision improvement, age-related macular degeneration.

1. Introduction

The first human trial of refractive surgery (PRK) was conducted by McDonald in 1988, based upon the IBM patent (UV laser for organic tissue ablation). FDA approval PRK in 1995 and LASIK in 2002. The flying-spot scanning method was invented by J.T. Lin in 1991 (US patents, 1991, 1993) who also introduced the first customized procedure in 1996. During 1995-1999, various laser systems/procedures were developed including: laser thermal keratoplasty (LTK) using Ho:YAG laser, DTK using diode laser, RF and CK designed for hyperopia corrections; solid state lasers (Nd:YAG-213 nm for PRK), Nd:YAG pico-second-PRK, Mini-Excimer for PRK etc. Technologies developed in the 2000's include: eye-tracking device (Lai, Novatek), microkeratome, elevation map, topography-guided LASIK, wavefront for customized LASIK (Tracey), presbyopia treatment using SEB (Schachar) and laser scleral-ablation for presbyopia (Lin); accommodative IOL. More recently, femto-second lasers are developed for corneal flat and stroma ablation, a procedure called SMILES. Review articles for refractive surgery are available in Refs [1-5].

Corneal collagen shrinkage has long been used in refractive surgery to change the shape and refractive properties of the cornea [2,3]. Recently, a new corneal procedure, corneal photovitrification (CPV), has produced changes in corneal shape and refractive

properties by treating corneal stromal tissue to reduce hydration and increase modulus [6,7]. CPV has been demonstrated to be safe and effective in providing vision improvement to eyes with age-related macular degeneration (AMD) and other retinal disorders [7]. Since laser irradiation of corneal tissue is part of the CPV treatment, it is desirable to understand the effects of laser irradiation parameters (pattern, wavelength, spatial and temporal irradiance, etc.) on treatment efficacy in order to optimize treatments. This paper presents an efficacy analysis of CPV treatments based on the rate equation for the CPV-treated corneal stroma and a rate coefficient given by an Arrhenius formula,

The CPV efficacy, in general, is both time and depth dependent due to the light intensity penetration depth in the tissues which is inverse proportional to the tissue absorption coefficient. Therefore, a "volume" efficacy is required to define an actual CPV conversion within the treated volume (area x depth). This new concept will be proposed in the present article. The CPV efficacy will be calculated based on a corneal stroma rate equation having a rate coefficient given by an Arrhenius formula. The temperature spatial and temporal profiles are given by the numerical solutions of a heat diffusion equation with a volume heating source. Various effective depths including the tissue damage depth, temperature penetration depth and conversion depth, governed by the tissue absorption coefficient, light intensity and dose (or irradiation time), and the related threshold values, are introduced in replacing the conventional penetration depth based on a simple Beer's law. The present modeling system with numerical data will be presented to provide quantitative guidance and/or predictions for the clinical aspects for our previous clinical studies [6,7].

2 Methods and Modeling Systems

2.1. Temperature rise

The temperature change of the cornea tissue (stroma) due to light heating can be described by a generalized heat diffusion equation [8-10]

$$\nabla^2 T(z,t) - \frac{1}{k'}\frac{\partial T(z,t)}{\partial t} = -S(z) \qquad (1.a)$$

where the laser heating source term, S(z) is given by

$$S(z,t) = \frac{A(t)I(z,t)}{K} e^{-Bz} \qquad (1.b)$$

k' and K are, respectively, the thermal conductivity and diffusivity of the tissue. B is the extinction coefficient of the cornea (at a specific laser wavelength), which consists of two components: B=[A (A+2b)]1/2, with A and b are the absorption and scattering coefficients, respectively. In this study, we will focus on the role of the absorption term (A), with b<<A, such that B=A in our calculations. We note that the absorption coefficient, A(t), in general is temperature-dependent. For example, A(in water) is given by A(T)=31.8-0.104(T-293) for a light wavelength at 2.09 um showing a decreasing function of T; whereas its is an increasing function of T for a light wavelength of 1.85 to 1.93 um [11,12]. The shorter wavelength light (1.4 to 1.84 offers an advantage of safety protection when the tissue temperature increases , and leads to a shorter penetration depth.

I(z,t) is the laser intensity without the absorbing medium, and in a general case for a focused laser beam is given by (for z<f), $I(z)=I_0/[1-(1-w)z/f]^2$, with w is spot size ratio of the beam on the corneal surface (z=0) and at the focal point (when z=f), with f being the focal length. For a collimated beam, w=1 and $I(z) = I_0$ is the surface constant light intensity. For a pulsed laser case, I(z,t) is also time-dependent, if multiple pulses are applied.

The above heat diffusion equation may be solved numerically under the initial condition: $T(z,0)=T_0$, and under the boundary condition (at z=0) [10]

$$[\frac{\partial T(z,t)}{\partial z}]_{z=0} = \frac{h}{K}[T(t,z=0) - T_0] \qquad (2)$$

where h is the heat transport coefficient due to the air convection or heat sink cooling window of the corneal surface. For a pulsed light heating case, the source term may be written as a Heaviside function, H(t), as S(z,t) =S(z)[H(t)-H(t-dt)], where dt is the pulse duration, or on-time.

In a cw (or long pulse) laser operation, the laser-heated solution will reach a steady-state when the irradiation time is much longer than the thermal relaxation time (Tr) given by [13] $Tr=179/A^2$ (in pure water) or $Tr=251/A^2$ (in tissue). For example, in the case of water solution, Tr= (179, 20, 0.8, 0.2) seconds for A =(1,3,15,30) cm^{-1}. For a constant absorption coefficient, A(t)=A, and a collimated light $I(z=0,t=0)=I_0$, the steady state solution, for dT/dt=0, is given by [8,10]:

$$T(z) = I_0\,(1 - e^{-Az})/(AK) - (I_0/K + G)z \qquad (3.a)$$

$$G = \frac{h}{K}[T_0 - T(t,z=0)] \qquad (3.b)$$

We note that the slope of T(z) is given by Eq, (2), which has an optimal z* given by when dT/dz (z=z*)=0, or $z^*=(1/A)\ \ln [1/(1+KG/I_0)]$. When a sapphire window is contacted to the corneal surface, it has a room temperature T (t,z=0) =20° C, the heat flows from the warmer cornea (at initial T_0 approximately 35° C) to the sapphire window such that G>0, initially and becomes G<0 later.

2.2. The CPV efficacy

The CPV efficacy (Ceff) is defined by $Ceff =1 - M(z,t)/M_0 =1-\exp(-S')$, where M_0 is the amount of initial corneal tissue prior to the light irradiation, and M(t) is the amount of modified corneal tissue after CPV, given by the solution of [14]

$$\frac{dM(z,t)}{dt} = -k(z,t)M(z,t) \qquad (4.a)$$

$$k(z,t) = A_0\exp(-E_a/[R(T+273)]) \qquad (4.b)$$

where k(z,t) is the rate coefficient given by an Arrhenius formula , Eq. (4.b), in which Ea (in J/mole) is the activation energy (for CPV to occur) and R [in J/(Kmole ^{0}C)] is the gas constant R=8.314(in J/mole/^{0}C, and T(t,z) is the temperature in ^{0}C. For cornea, the Arrhenius parameters are selected to be: $A_0=3.0\times10^{44}\ sec^{-1}$, Ea =293 kJ/mole. Therefore Ceff=1-exp(-S'), with S' is the time integral of k(z,t).

The Ceff, In general, is both time (t) and depth (z) dependent due the light intensity penetration depth in the tissues which is inverse proportional to the tissue absorption coefficient. Therefore, a "volume" efficacy is required to define an actual conversion within the volume (area x depth) of light acting soft tissues. This is a new concept proposed in the present article. More details will be discussed later.

3. **Results and discussions**

We have previously published the numerical results for a anti-cancer lasers system [15] using nanogold as the absorber, in which a diode laser at 808 nm was used having laser irradiation time is about few minutes due to the rather low absorption coefficient of nanogold at about A= 3 to 5 cm^{-1} and a penetration depth (Z_P) about Z_P=1/A=0.2 to 0.33 cm. A

temperature increase of about 10 to 15 ^{0}C is required to kill the cancer cells. In comparison, in a corneal system under laser thermal effects, much higher A= 20 to 100 cm^{-1} and Z_P= 0.1 to 0.5 mm are involved and therefore, a shorter irradiation time of about 100 to 500 ms is required for a temperature increase of about 20 to 50 ^{0}C. The numerical solutions of Eq. (1) and (4) require the information of the related parameters and properties of the heated corneal tissue. The present article will focus on the simplified and/or limiting cases such that analytic formulas are available for key features of CPV. The numerical data of anti-cancer system will be scaled (in time and depth) proportionally to present the trends/features of corneal systems [6,7] without repeating the complex numerical simulations (which will be shown elsewhere).

3.1 Temperature profiles

Fig. 1 shows the calculated surface temperature profiles T(t, z=0). For a fixed absorption coefficient (left figure), the temperature profiles has faster rising curve for higher laser intensity. Similarly, for a fixed I, it is a faster rising curve for higher A (right figure).

Fig. 2 shows the surface temperature profiles T(t, z=0) are increasing function of A and I_0, and the steady-state saturated profiles can be described by Eq. (3).

Fig. 3 shows the calculated temperature spatial profiles T(z) at a given laser irradiation time of 250 ms for various A=(15, 30,60) cm^{-1}, with a fixed I_0=200 W/cm^2. It shows that higher A leads to a higher peak temperature, but a smaller penetration depth, which is also demonstrated by Eq. (3).

Fig. 4 shows the effect of heat transport coefficient (G). For a fixed A and I_0, the temperature spatial profiles T(z) are decreasing function of z and G. We note that G is also related to the cooling window contacted to the corneal surface.

Fig. 5 shows the irradiation time needed (t') for the corneal surface to reach a temperature of 80 ^{0}C, for various A=(30,40,90) cm^{-1}. It shows that t' is a decreasing function of A and I_0. Therefore, to reach a desired temperature, one may adjust the irradiation time (from 0.1 to 0.5 s) for a fixed laser intensity; or adjusted the intensity (from 100 to 200 W/cm^2) for a fixed A (or laser wavelength).

Fig. 6 shows the calculated surface temperature profiles T(t, z=0) under a pulsed (on-off) laser with various off-time and a fixed on time [10]. It shows that T(t,z) is a decreasing function of the off-time due to the heat transport during the off-period in consistent with measured data [16]. This controlled pulsed laser method can be tailored to optimize the efficacy and avoid surface damage, besides the use of cooling window.

We note that the information provided by Figs. 1 to 6 provides the guidance to choose an appropriate laser wavelength (which also defines A), such that the desired surface (and volume) temperature could be reached by adjusting the combined parameters of (I_0, t'), with I_0= (50 to 200) W/cm^2, and t'=(0.1 to 1.0 s). However, to protect the corneal surface layer, the appropriate laser wavelength must be in the range of 1.42 to about 2.2 um, having A= 15 to 100 cm^{-1}, such that the penetration depth (approximately given by 1/A) is in the range of 100 to 650 um.

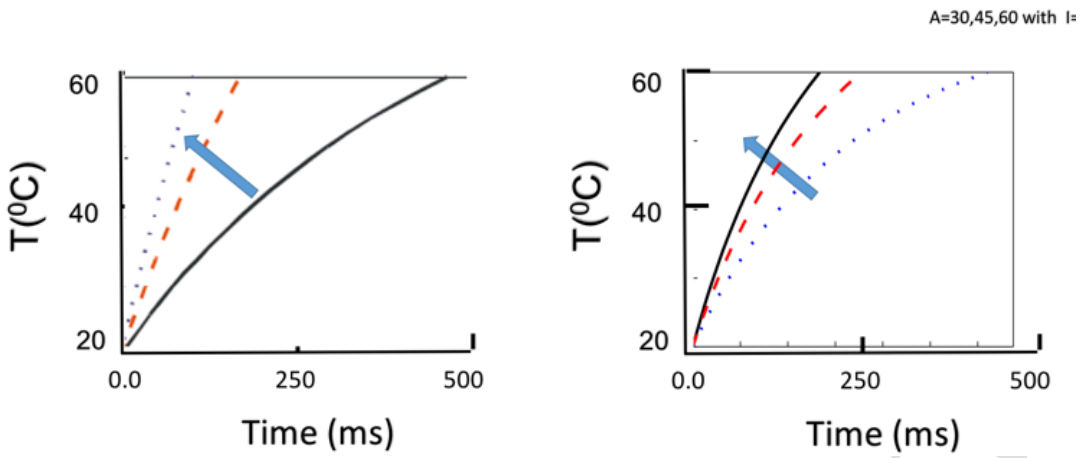

Fig. 1 Calculated surface temperature profiles T(z=0) (Left) for the effects of laser intensity, I_0=(50,100,200) W/cm^2, for curves right to left, for a fixed A=60 cm^{-1}. (Right) temperature profiles for a fixed I_0=100 W/cm^2, but for various A=(30,45,60) cm^{-1}, for curves right to left.

Fig. 1 Calculated surface temperature profiles T(z=0) (Left) for the effects of laser intensity, I_0=(50,100,200) W/cm^2, for a fixed A=60 cm^{-1}. (Right) temperature profiles for a fixed I_0=200 W/cm^2, but for various A=(30,45,60) cm^{-1}.

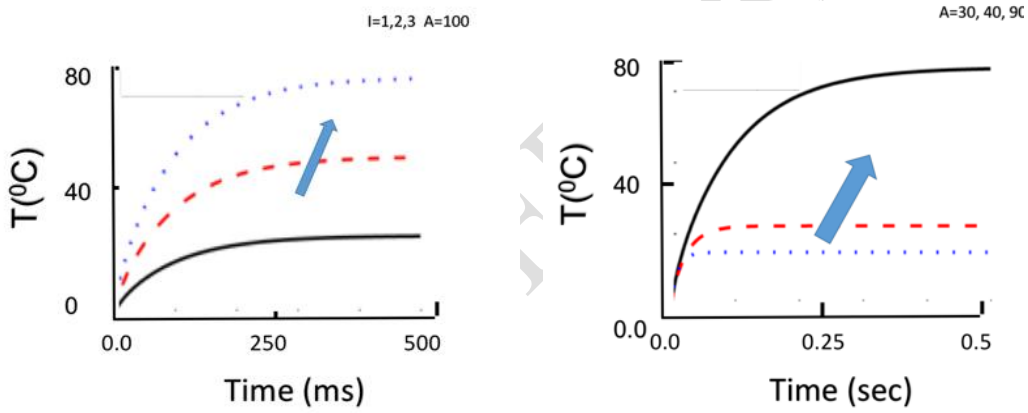

Fig. 2 Calculated surface temperature profiles T(z=0) (Left) for the effects of laser intensity, I_0=(50,100,200) W/cm^2, for curves low to top, for a fixed A=90 cm^{-1}; and (right) for various A=(30,40,90) cm^{-1}, for curves low to top, with a fixed I_0=200 W/cm^2.

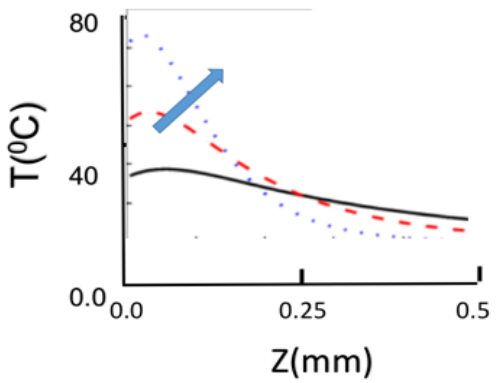

Fig. 3 Calculated temperature spatial profiles T(z) at a given laser irradiation time (t=500 ms) for A=(15, 30,60) cm^{-1}, for curves low to top with a fixed I_0=200 W/cm^2, and heat transport coefficient range of G= 0.5 WC/cm^2.

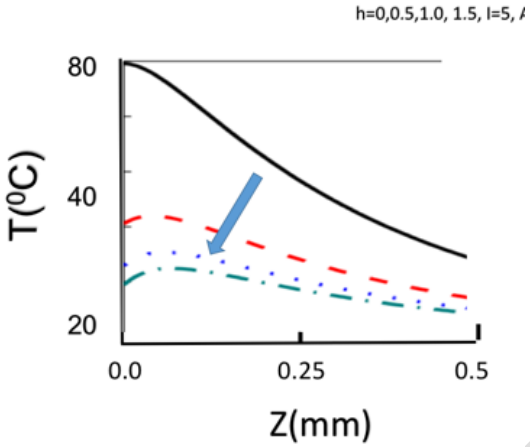

Fig. 4 Calculated temperature spatial profiles T(z) at a given laser irradiation time (t=500 ms) for heat transport coefficient range of G= (0, 0.5, 1.0, 1.5) WC/cm^2, for curves top to low, with fixed A=60 cm^{-1} and I_0=200 W/cm^2.

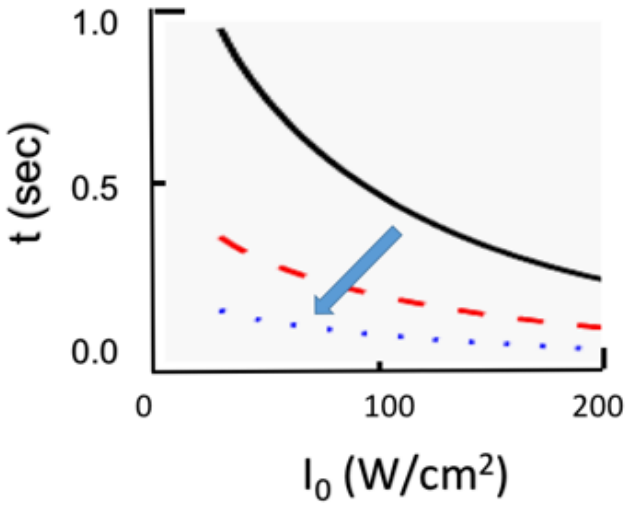

Fig. 5 The calculated irradiation time needed (t) to reach a surface temperature of 60 ^{0}C, for various A=(30,40,90) cm^{-1}, for curves from top to low, for an irradiation time of 0.5 s.

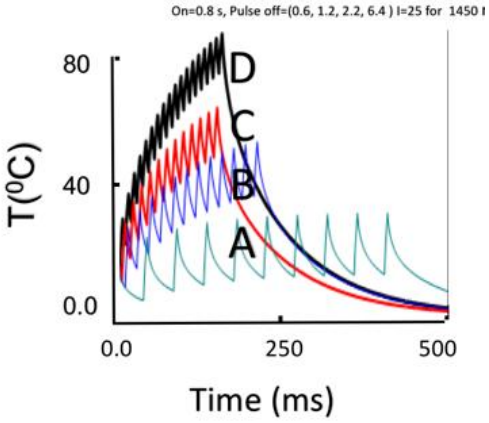

Fig. 6 Calculated surface temperature profiles in water using a pulsed diode laser at 1450 nm for laser intensity I_0 =5 (W/cm^2) and laser on-time of 0.2 sec with various off-time of (0.15, 0.3, 0.5, 1.5) sec, for curves (A,B,C,D), respectively. [10]

3.2 Effective depths

The conventional definition of light penetration depth (z') is based on the Beer's law exp(-Az), when Az=1, or z'=1/A, which is an inverse function of the absorption coefficient (A). However, this simple definition can not describe the complete features of measured parameters such as the tissue damage depth (Z_D), temperature penetration depth (Z_T), and conversion depth (Z_C), which are governed by the parameters of light intensity and light dose (or irradiation time), and the related threshold values, besides the absorption coefficient (A). We propose the more rigorous definitions for Z_D, Z_T and Z_C as follows.

As shown in Fig. 7, the temperature spatial profiles for various absorption coefficient (A), at a given irradiation time and under a cooling window for an initial surface temperature about 20 ^{0}C. Fig. 7 shows the following features:

(i) Larger A (shown by Curve-A) leads to a higher peak temperature, but a smaller temperature penetration depth (Z_T) defined by T(z=Z_T) =T(peak), which is approximately given by 1/A.
(ii) The tissue damage depth (Z_D) is defined by a threshold damage temperature (T1), therefore, large A (Curve-A) with a small Z_D has a better protection of the posterior layer (at about 500 um) than that of small A (Curve-B and C), but it damages the anterior layer (Z1, about 70 um). In contrast, Curve-C (with the smallest A) protects the anterior layer, but not the posterior layer. Curve-B having an optimal A protects both anterior and posterior layers.
(iii) The conversion depth (Z_C) is defined by threshold conversion temperature (T2) such that the rate constant, k(t,z=Z_C) is high enough to achieve a threshold efficacy and at depth Z_C.

We note that the above discussed depths are all inverse proportional to A, but the exact relationship requires numerical calculation of T(z,t), and they are also function of the light intensity and irradiation time (or light dose) having a nonlinear power. For example, the irradiation time must be sufficiently short to prevent overheating of anterior and posterior layers and localize the temperature rise within the corneal stroma (or T1<T<T2 for z<ZD,), but long enough to achieve the conversion threshold depth (Z_C) for a given optimal A. More details of Z_C will be discussed later.

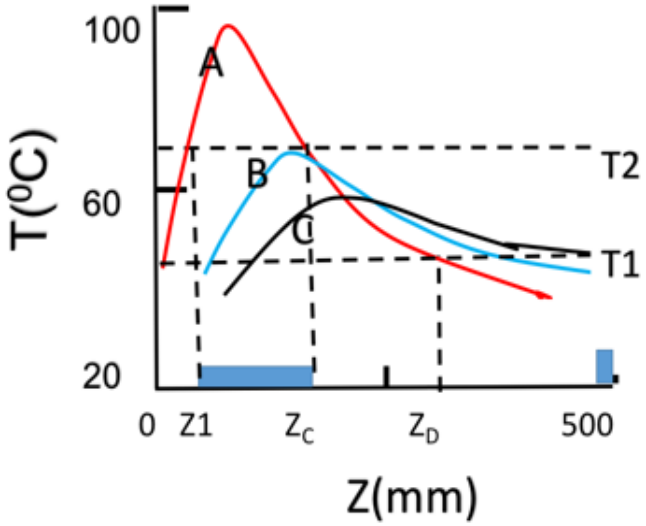

Fig. 7 Calculated temperature spatial profiles (at irradiation time t=250 ms) for various A=(30,60,90) cm^{-1} for Curve-C, -B, -A, and a fixed I_0=3 W/cm^2.

3.3 CPV efficacy

To calculate the CPV volume efficacy, one requires the temperature spatial (Fig. 7) and temporal (Fig. 8) profiles and the related temperatures T1, T2, and T3; and the depths of Z1, Z_C and Z_D. The CPV volume efficacy is given by the double integral of k(z,t), for time integral of t=t1 to t2 (shown by Fig. 8) and the spatial integral of z=Z1 to Z_C (as shown by Fig. 7). As defined earlier (referred to Fig. 7) that the conversion depth (Z_C) is defined by threshold conversion temperature (T2) such that the rate constant, k(t,z=Z_C) is high enough to achieve a threshold efficacy and at depth Z_C. Numerical integration of k(z,t) is needed, even when the analytic solution of T(z,t) is given, and it will be presented elsewhere. However, Fig. 7 and Fig 8 provide us comprehensive features s follows:

(i) For efficient conversion (with Ceff >0.6), as shown by Fig. 7, large A (Curve-A) leads to a small Z_D has a better protection of the posterior layer (at about 500 um) than that of small A, but it also leads to a smaller volume Ceff. Therefore optimal A is required for deep z>Z_C, with T (at z=Z_C) >T2, for maximum Ceff, but small z<Z_D with T (at z=Z_D)<T1 to avoid posterior damage.

(ii) As shown by Fig. 8, for efficient conversion, large A, shown by Curve-A, is needed such that (t2-t1) is maximum for maximum volume Ceff, which is proportional to the time integral of k(z,t) over t1 to t2. The Ceff (z,t) also increasing function of the light irradiation time, which should be long enough (for large t2 and T>T2), but short enough (with T<T1 at z=Z_D) to avoid the posterior damage. For example, if a conversion corneal stroma depth of 150 um is desired, parameters of A about 80 cm^{-1} t abut 150 ms, for a spot diameter of 5.0 mm (or intensity is 1.53 W/cm^2), and laser dose about 250 mJ/cm^2 are required. In comparison, for the case of deep sclera softening (about 500 um), parameters of A about 20 (1/cm), t about 500 ms, and I_0 about 3.0 W/cm^2 are required. These theoretically predicted/proposed parameters, however, need further confirmation by measure data.

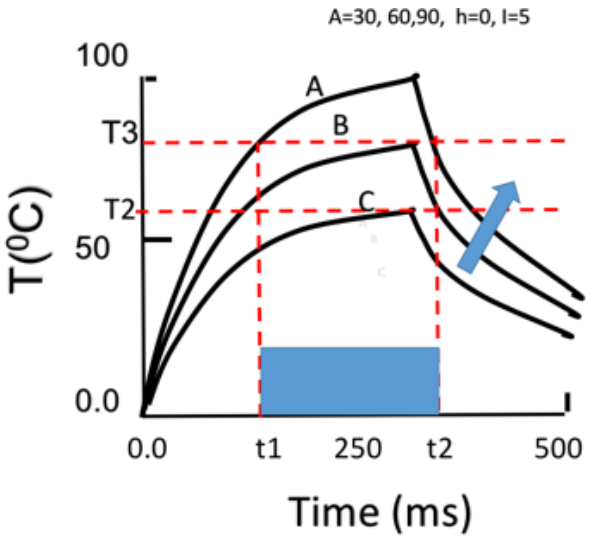

Fig. 8 Calculated surface temperature (at z=0) profiles for various A=(30,60,90) cm^{-1} for Curve-C, -B, -A, and a fixed I_0=3 W/cm^2, where T1 (t1) and T2 (t2) define the temperature range of efficient CPV.

3.4 Surface damage and cooling

Besides the use of pulse mode (as shown by Fig. 6) to reduce the corneal surface temperature and avoid the damage, a pulsed-train technique was also proposed by Lin for increased volume temperature without over heating the tissue surface [13].

The heat sink cooling process may be passive such as the use of dynamic cooling performed pre-laser and/or intra-laser irradiation [16]. Sapphire or other material(s) may be used for this heat sink application in the transparent window. Based on the thermal properties of sapphire and cornea [9], we found that during light irradiation of the cornea (about 200 ms), the "thermal depth" could be approximately 80 μm for the cornea and approximately 760 μm for sapphire. Since thermal diffusion is more rapid in sapphire compared to the cornea, heat transfer is "rate-limited" by thermal diffusion through the cornea.

The range of thermal damage (i.e., cellular necrosis due to heating) to each in vivo corneal structure within each treated volume including the corneal basal epithelium is limited to thermal damage between 1% to 50%. As an example, our previous [9] study showed that if the fast heating duration at maximum temperature (T_{max}) is 1.0 second, T_{max} can be 49.2° C. if 0.1% thermal damage is acceptable but can be a greater T_{max} of 56.2° C. if 1% thermal damage is acceptable (and 63.4° C. if 10% thermal damage is acceptable). In addition, only the center of the heat affected zone (HAZ), is heated to T_{max}; other portions of the HAZ are heated to temperatures less than T_{max}. Because rate processes occur with rate coefficients that increase exponentially with increasing T, treatment occurs predominantly in a treated volume the corneal modification can be a corneal vitrification, wherein the corneal vitrification can be maximized, and thermal damage can be minimized.

When a sapphire window (at room temperature T_0=approximately 20° C.) contacts the cornea (at physiological temperature T_p=approximately 35° C., although this varies as a function of age, room temperature, and so on), heat flows from the warmer cornea into the cooler heat sink. This heat transfer case is similar to the case of a semi-infinite solid (the cornea and the rest of the body behind it) bounded at its anterior surface (z=0, the tear film/anterior epithelium) by a heat sink kept at a fixed temperature T_0. As shown by Fig. 8, the temperature rise spatial profiles (at a given light irradiation time about 200 ms) having a lower temperature near the surface (for z<Z1), and a peak value at $z=Z_C$. for bare cornea and for cornea in contact with a sapphire window.

It was reported [11,12] that the absorption coefficient, A, in general is temperature-dependent. For example, as shown by Fig. 9, A (in water) is given by A(T)=31.8-0.104(T-293) for a light wavelength at 2.09 um showing a decreasing function of T; whereas A is an increasing function of T for a light wavelength of 1.85 to 1.93 um [11] which offers a safety protection by a smaller penetration depth at higher temperature. For light wavelength in the range of 1.86 um to 1.9 um, the posterior layer can be protected when temperature reaches about 70 ^{0}C, where the light penetration is limited to about 150 um depth and it is desired for applications require a shallow penetration. However, for applications require deeper penetration of 500 to 600 um (such as sclera heating), light wavelength with a smaller absorption coefficient (with A <301/cm). or having A is a decreasing function of temperature is desired, such as in the range of 1.45 to 1.48 um or 1.95 to 2.1 um, which however has less posterior protection.

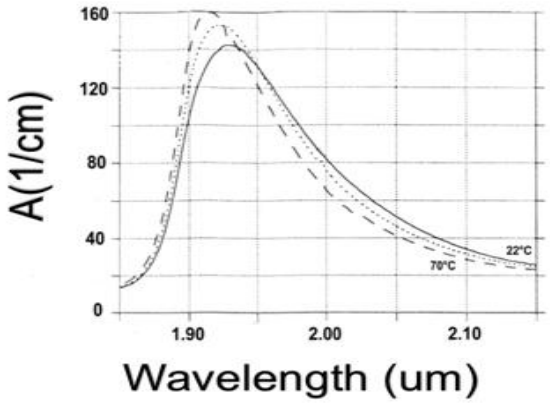

Fig. 9 Water absorption spectra at different temperatures (solid: 22°C, dotted: 49°C, dashed: 70°C), after Ref. [11].

4. Clinical aspects and analysis

We will now analyze our clinical data [6,7] completed using the Clear-K® Low Vision Aid System (Optimal Acuity Corporation, Austin, TX) based on our mathematical model and the numerical analysis of temperature rise and various effective depths described in Section 3.2: the tissue damage depth (Z_D), temperature penetration depth (Z_T), and conversion depth (Z_C). These depths are governed by the parameters of light intensity and light dose (or irradiation time), and the related threshold values, besides the absorption coefficient (A).

As discussed earlier the CPV efficacy, Ceff, is given by the solution of Eq. (4) or the time integral of a rate coefficient, k(z,t), which is related to the temperature by an an Arrhenius formula. The CPV efficacy, In general, is both time (t) and depth (z) dependent due the light intensity penetration depth in the tissues which is inverse proportional to the tissue absorption coefficient. Our modeling system having numerical data shown by Figs. 1 to 9, provide quantitative guidance and/or predictions for the following clinical aspects for our previous clinical studies in animal and human. [6,7]

CPV treatment safety and efficacy depend upon:

– laser parameters (intensity, spot size, wavelength);
– corneal response: the tissue damage depth (Z_D), temperature penetration depth (Z_T);
- CPB efficacy: depends on the temperature rise, the conversion depth (Z_C) and the time integral of a rate coefficient, k(z,t);
- clinical protocol (laser irradiation time, treatment area and spot size)
- mechanisms of action for vision improvement, which also define the rate coefficient, k(z,t);

– long-term effects, including evolution of corneal changes.

4.1 Safety and Efficacy

For safety, CPV treatment does not produce serious adverse events (SAEs) or complications, including discomfort, diplopia or dysphotopsia (glare, halo, etc.). SAEs include corneal perforation, corneal scarring and persistent corneal epithelial defect. The safety issue is discussed by the tissue damage depth (Z_D) which is further defined by a threshold damage temperature (T1); and a large A (Curve-A) leads to a small Z_D has a better protection of the posterior but it damages the anterior layer (about 70 um). To overcome the surface layer damage under a laser having a large A (about 60 to 100 cm^{-1}), a sapphire window (at about 20° C) was used as a heat sink to protect the cornea (having an initial physiological temperature about 35° C), such that the tear film/anterior epithelium by a heat sink kept at a fixed temperature T_0, having a lower temperature near the surface (for z<Z1), and a peak value at $z=Z_C$, as demonstrated by Fig. 8.

We have previously measured the histology for a diode laser (at about 1.9 um) delivered by a fiber with core diameter of 500 µm to a porcine cornea contacted with a 1 mm thick sapphire window for epithelium cooling. The heated effective zone is approximately 400µm diameter and 100µm deep in the center. This penetration depth is also predicted by our temperature penetration depth (Z_T) defined by $T(Z_T)=T(peak)$, which is approximately given by 1/A, and Z_T =100 µm, for A=100 cm^{-1} (for laser at about 2.0 µm). For efficacy, CPV treatment should produce maximum vision improvement as rapidly as possible after treatment and the vision improvement should have a long duration of effect. the short term CPV efficacy is given by Ceff (z,t) = 1 - $M(z,t)/M_0$, and M(z,t) is given by the solution of the rate eq. (4). The "volume" efficacy is proportional to the heated effective zone volume (or area x depth).

4.2 Proposed Mechanisms

The long term outcomes are defined by the tissue long term response including possible post-treatment regressions, in which the CPV mechanism plays the critical role. We have previously proposed that the treated corneal stromal has reduced hydration and increase modulus leading to changes in corneal shape and refractive properties. The proposed mechanisms are discussed as follows.

The mechanism of action of vision improvement by CPV treatment probably involves both optical and neuroadaptation effects. Optically, the corneal shape and refraction changes due to CPV treatment cause redistribution of irradiance on the retina. However, from retinal spot diagram measurements (using an iTrace analyzer), it appears that the average irradiance redistribution is about 40 µm [6], and this is not large enough to cause major relocation of the preferred retinal locus (PRL). The optical effect is minor and microperimeter measurements (see below) show that the PRL moves very differently from patient to patient although all patients received the same treatment. The optical effect is not similar to that produced by prism spectacles (that cause consistent changes from patient to patient when the same prism orientation and magnitude are used). In addition, no eye movement training was done to cause PRL movement; in fact, most patient PRLs continued to move at multiple examination times (*e.g.*, from 1 to 3 to 6 to 12 months post-treatment) – this is evidence for continuing neuroadaptation over time.

We have also studied the neuroadaptation effects by microperimeter images and retinal sensitivity measurements of the treated CPV eyes. As shown by Fig. 10, at 1 month post-CPV, the distribution of fixation points (blue-green dots in the figure) was centered superiorly with respect to the atrophic retina; this corresponds to a PRL relocation of about 1.0 mm on the retina. Retinal sensitivity measurements (shown in color coding at 37 stimulus points over 10° diameter, about 3.0 mm diameter), the black (zero sensitivity) stimulus points overlap the atrophic retina. The distribution of fixation points moved from overlap with the atrophic area (pre-CPV) superiorly onto a more functional retina (1m post-CPV).

It is postulated that the large PRL movement observed at 1m post-CPV is caused mainly by neuroadaptation including an oculomotor response that changes the eye's gaze. It is typical that pre-CPV eyes with AMD have PRLs that overlap atrophic regions of the retina, including the dysfunctional fovea. It is postulated that these patient PRLs are "stuck" in the locations that the patients have used during their lives prior to loss of central vision and that new information is required to "unstick" the PRLs from the old location to a more functional new location. Further investigation is needed to determine the CPV treatment mechanism of action.

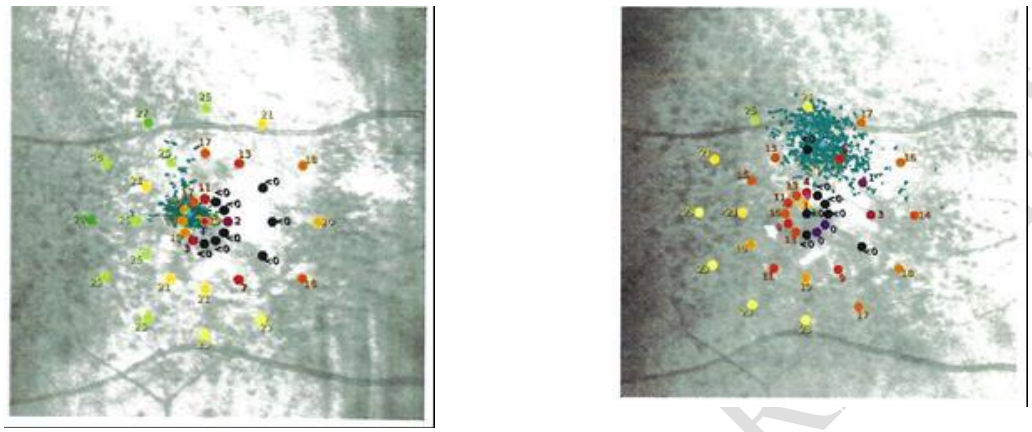

Fig. 10. Microperimeter images for one eye. Left – pre-CPV, right – 1m post-CPV. The distribution of fixation points is shown by the blue-green dots. After Ref.[7].

4.3 Suggested protocols

Clinical observations (fluorescein staining of corneal epithelia) have been used to determine the maximum laser dose (intensity x irradiation time) that retains an undamaged epithelium [7]. For our current CPV treatments, a diode laser at about 2 μm wavelength (with A about 100 cm^{-1}), and it is about 50 mJ/spot energy for 4 spots (diameter of 0.6 mm) at the symmetric positions of 45, 135, 225 and 315 degrees. The irradiation was completed through a sapphire window with one mm thickness were used. The laser dose is calculated to be about 230 mJ/cm^2/spot, for a laser power of 0.33 W with spot diameter of 0.5 mm (or intensity is 170 W/cm^2), and irradiation time of 150 ms, 170x150/1000=25.5 J/cm^2). We note that the damage threshold is defined by the dose, or energy per unit area (and depends on the spot size), rather than the energy or power (which is independent to the spot size). A new diagnostic examination, the potential visual acuity (PVA) test [17], is now available for determining patient eligibility for achieving significant vision improvement. The PVA test should be useful clinically for screening good candidates for CPV treatment.

No post-CPV care is required but patients are advised to practice their distance vision by looking at objects such as street signs and trees and to practice their near vision by reading and doing other near vision tasks. Patients are also advised to protect their eyes from risks such as sunlight without sunglasses and from bright lights in general and to avoid other risk factors such as smoking. Patients are also advised, depending on their stage of AMD, to take AREDS 2 supplements [17] or, perhaps better, higher doses of carotenoids such as lutein and zeaxanthin [18]. Some earlier background about AMD can be found in Refs. [19] and [20].

5. Conclusion

CPV treatment safety and efficacy depend upon: laser parameters (intensity, spot size, wavelength), the tissue damage depth (Z_D), temperature penetration depth (Z_T), the conversion depth (Z_C), and the time (t) and depth (z) integral of a rate coefficient, k(z,t),

given by an Arrhenius formula. The suggested protocol for our current CPV treatments include: a diode laser at about 1.9 μm wavelength (with A about 100 cm^{-1}) which is delivered to the corneal surface by a 1-to-4 fiber splitter (with fiber core of 500 μm) and a 1.0 mm sapphire cooling window. The laser dose is about 25.5 J/cm^2/spot, for a laser power of 0.33 W with spot diameter of 0.4 mm and irradiation time of 150 ms. The microperimeter images and retinal sensitivity measurements of the treated CPV eyes demonstrated that the large PRL movement observed post-CPV is caused mainly by neuroadaptation including an oculomotor response that changes the eye's gaze.

REFERENCES

1. Lin JT. Critical review on refractive surgical lasers. Optical Engineering, 1995, 668-675.
2. Lin JT. Progress of the 30-year laser vision technology. J Ophthalmol Clinical Res . 2017:3:1-4.
3. Reinstein DZ, Archer TJ, Gobbe M. The history of LASIK. J Refract Surg 2012;28:291-298.
4. Kim T, Alio JL, Wilkins M, et al. Refractive surgery. The Lancet, 2019, 393, 2085-2098.
5. Ang M, Gatinel D, Reinstein DZ, *et al.* Refractive surgery beyond 2020. Eye, 2021, 35, 362–382. https://doi.org/10.1038/s41433-020-1096-5.
6. Stein RM, Markowitz SN, Berry M *et al.* Corneal laser procedure for vision improvement in patients with late stage dry age-related macular degeneration - a retrospective observational cohort study. F1000Research, 2020, 9:1500.
7. Devenyl R, Markowitz SN, Berry II M. *et al.* Corneal laser procedure for vision improvement in patients with neovascular age-related macular degeneration and other retinal disorders involving central vision loss: a retrospective cohort study F1000Research, 2022, 11:316.
8. Carsiaw HS and Jaeger JC. Conduction of Heat in Solids. 2a Edition (Oxford University Press, London, 1959).
9. Valderrama GL, Fredin LG, Berry MJ. *et al*. Temperature distribution in laser-irradiated tissues. SPIE 1991,1427:200-213.
10. Lin JT. Design of clinical procedures using diode lasers operated in continuous wave and pulsed modes. Medical Device Diagn Eng. 2016;1: 29-35.
11. Jansen ED, van Leeuwen TG, Motamedi M et al. Temperature dependence of the absorption coefficient of water for midinfrared laser radiation. Lasers Surg Med. 1994;14:258-268
12. Lange BI, Brendel T, Hüttmann G. Temperature dependence of light absorption in water at holmium and thulium laser wavelengths. Appl Opt 2002;41:5797-5803.
13. Niemz NH. Laser-tissue interactions: Fundamentals and applications, Springer-Verlag: Heidelberg, 2004.
14. Lin JT, Cheng, DC. Modeling the efficacy profiles of UV-light activated corneal collagen crosslinking. PloS One. 2017;12:e0175002.
15. Lin JT, Chiang S, Lin GH, Liu HW. In vitro photothermal destruction of cancer cells using gold nanorods and pulsed-train near-infrared lase. J. Nanomaterials. 2012; article ID 861385.
16. Zhang R, Ramirez-San-Juan JC, Choi B, et. al., Thermal responses of ex vivo human skin during multiple cryogen spurts and 1,450 nm laser pulses. Laser Surg Med. 2006,38:137-141.
17. Lem DW, Davey PG, Giethart DL et al.*et al*. A systematic review of carotenoids in the management of age-related macular degeneration. Antioxidants 2021;10:1255. doi: 10.3390/antiox10081255.
18. https://www.nei.nih.gov/learn-about-eye-health/eye-conditions-and-diseases/age-related-macular-degeneration/nutritional-supplements-age-related-macular-

degeneration.
19. Gehrs KM, Jackson JR, Brown EN Allikmets R, Hageman GS. Complement, age-related macular degeneration and a vision of the future. Archives of ophthalmology. 2010, 128:349-58.
20. Berdeaux GH, Nordmann JP, Colin E, Arnould B. Vision-related quality of life in patients suffering from age-related macular degeneration. American journal of ophthalmology. 2005, 139:271-9.